

Research Article

Distributed Multistatic Sky-Wave Over-the-Horizon Radar's Positioning Algorithm for the Marine Target

Fangyu Ren , Huotao Gao , Lijuan Yang , and Sang Zhou 

Electronic Information School, Wuhan University, Wuhan 430072, China

Correspondence should be addressed to Huotao Gao; gaoght863@163.com

Received 6 August 2021; Accepted 15 October 2021; Published 27 October 2021

Academic Editor: Atsushi Mase

Copyright © 2021 Fangyu Ren et al. This is an open access article distributed under the Creative Commons Attribution License, which permits unrestricted use, distribution, and reproduction in any medium, provided the original work is properly cited.

This paper establishes a distributed multistatic sky-wave over-the-horizon radar (DMOTHR) model and proposes a semidefinite relaxation positioning (SDP) algorithm to locate marine ship targets. In the DMOTHR, it is difficult to locate the target due to the complexity of the signal path propagation. Therefore, this paper uses the ionosphere as the reflector to convert the propagation path from a polyline to a straight line for establishing the model, and then the SDP algorithm will be used to transform a highly nonlinear positioning optimization problem into a convex optimization problem. Finally, it is concluded through the simulations that the SDP algorithm can obtain better positioning accuracy under a certain Doppler frequency error and ionospheric measurement error.

1. Introduction

In the DMOTHR, OTHR can usually cover surveillance areas outside the range of conventional line-of-sight radars due to the refraction and reflection of radio waves by the ionosphere [1, 2], so it can effectively monitor low-altitude flying objects and marine ship targets [3]. However, the propagation of sky-wave signals in the ionosphere will generate multipath signals [4], which pose a challenge to achieve target positioning. The positioning performance of the DMOTHR is related to the ionospheric state. The current models describing the ionospheric state are usually divided into the following three models: the multi-quasi-parabolic model (MQP), the Chapman ionospheric model, and the international reference ionosphere (IRI) model. At present, the MQP model is the most widely used in the DMOTHR [5], so the MQP model is used to describe the propagation path of the signal through the ionosphere in this paper.

Basically, conventional multistatic line-of-sight radars can adopt many methods for target positioning, such as time difference of arrival (TDOA), frequency difference of arrival (FDOA), and gain ratios of arrival (GROA) [6–10],

but it is not easy to achieve accurate target positioning by these methods because of the complexity of the signal propagation path in the OTHR. There are only few studies on the target positioning of the OTHR. Through the multipath propagation of the OTHR signal and the two-dimensional (2D) array structure, the joint estimation of the target position and height is solved [4], but this paper is only applicable to the 2D situation, and the target position in the actual geodetic coordinates cannot be estimated. The hill climbing algorithm based on the weighted least square method is used to locate the target of the OTHR [5]. This paper enriches the positioning method of the OTHR to a certain extent, but it only uses the time of arrival (TOA) for positioning; there may be a large error in positioning accuracy. In [11], the estimated multicomponent Doppler feature is used to track the instantaneous height of the maneuvering target. In the DMOTHR, this method can only get the instantaneous height of the target in the air, but not the precise position of the target. In this article, it can locate the marine target based on the Doppler frequency in the DMOTHR.

The errors caused by the positioning of the measurement parameters will also affect the positioning accuracy in many

cases. It is necessary to reduce the impact of such errors. A positioning method is proposed to reduce the estimation error by considering the position error of the receiver [12]. Under certain mild conditions, it can be close to the CRLB of the far-field source. Target positioning is carried out by using the TDOA of multiple incompatible sources and the position of the observation station, and the hypothetical source position is introduced to establish a closed model, which can realize that the measurement noise error and the position error of the observation station are small enough, and the condition of the CRLB can also be achieved [13].

Herein, the positioning optimization problem based on Doppler frequency is obtained by establishing the signal model of OTHR in this paper. On the one hand, the general positioning optimization algorithms can only get the local optimal solution [14, 15], and it is difficult to get the global optimal solution. In this article, the SDP algorithm is used, and the local optimal solution it obtained is the global optimal solution [16]. On the other hand, most of the Doppler frequency positioning algorithms can only use the grid search method in the existing literature [16], which inevitably brings about the problem of a large amount of calculation. The use of the SDP algorithm can solve the divergence problem and avoid a large amount of calculation [17–21]. Therefore, this paper uses the SDP algorithm to convert the highly nonlinear positioning optimization problem into a convex optimization problem and solve it. Within a certain measurement error range, it is concluded that the SDP algorithm has better positioning accuracy.

2. Signal Model

In the DMOTHR, M_1 moving transmitters, M_2 moving receivers, and a stationary ship target are distributed in this paper. The moving trajectory and moving speed of the stations are known. The transmitting stations both transmit and receive signals. After the transmitting stations transmit the signal, the receiving stations start to observe the target signal at regular intervals. In order to simplify the signal propagation path, this paper uses an equivalent diagram to represent the path propagation. Using the ionosphere as the reflecting surface, the transmitting stations and the receiving stations are mirrored to produce virtual stations, and the propagation path of the signal is shown in Figure 1.

There are $L = M_1 + M_2$ moving receiving stations (because the transmitter transmits and receives signals, the transmitter can be regarded as a receiver when processing the received signal) and a stationary target. After a short time interval, each receiving station receives the target signal once. It is assumed that each receiving station receives N target signal measurements, so a total of $M = LN$ Doppler measurements can be obtained. Then, the Doppler frequency measurement value can be expressed as

$$f_d = \frac{f_c}{c} \cdot \frac{\mathbf{v}_i^{blh} (\mathbf{u}_{BLH}^o - \mathbf{a}_i^{blh})}{\|\mathbf{u}_{BLH}^o - \mathbf{a}_i^{blh}\|} + \varepsilon_i, \quad i = 1, \dots, M, \quad (1)$$

where the target position is \mathbf{u}_{BLH}^o , \mathbf{a}_i^{blh} (the position latitude and longitude of the virtual station are the same as the real

station, and the altitude is twice the height of the ionosphere) is the coordinates of the virtual observatory, the speed of the virtual observatory is \mathbf{v}_i^{blh} (the virtual station has the same speed as the real station), the original carrier frequency of the signal is f_c , c is the signal propagation rate, and ε_i is the measurement error.

Let $f_i \triangleq c f_d / f_c$ and $n_i = c \varepsilon_i / f_c$, so the normalized Doppler frequency f_i is

$$f_i = \frac{\mathbf{v}_i^{blh} (\mathbf{u}_{BLH}^o - \mathbf{a}_i^{blh})}{\|\mathbf{u}_{BLH}^o - \mathbf{a}_i^{blh}\|} + n_i, \quad i = 1, \dots, M, \quad (2)$$

where n_i is the measurement noise. Next, $\mathbf{n} = [n_1, \dots, n_M]$ can be obtained by combining all the measured noises into a Gaussian random variable \mathbf{n} with zero mean; then, $\mathbf{Q}_d = E[\mathbf{n}\mathbf{n}^T]$ is the covariance matrix. Similarly, if the Doppler frequency measurement values are also combined into a vector $\mathbf{f} = [f_1, \dots, f_M]^T$, the conditional probability density function of the vector relative to the target position can be expressed as

$$p(\mathbf{f} | \mathbf{u}) = \frac{1}{(2\pi)^M \sqrt{|\mathbf{Q}_d|}} \exp\left\{-\frac{1}{2}(\mathbf{f} - \mathbf{f}^o(\mathbf{u}))^T \mathbf{Q}_d^{-1} (\mathbf{f} - \mathbf{f}^o(\mathbf{u}))\right\}, \quad (3)$$

where

$$\mathbf{f}^o(\mathbf{u}) = [f_1^o(\mathbf{u}), \dots, f_M^o(\mathbf{u})]^T,$$

$$f_i^o(\mathbf{u}) = \frac{\mathbf{v}_i^{blh} (\mathbf{u}_{BLH} - \mathbf{a}_i^{blh})}{\|\mathbf{u}_{BLH} - \mathbf{a}_i^{blh}\|}, \quad i = 1, \dots, M. \quad (4)$$

Then, the ML estimate of the target position \mathbf{u} can also be obtained as

$$\min_{\mathbf{u}} (\mathbf{f} - \mathbf{f}^o(\mathbf{u}))^T \mathbf{Q}_d^{-1} (\mathbf{f} - \mathbf{f}^o(\mathbf{u})). \quad (5)$$

According to equation (3), the FIM matrix of \mathbf{u} can be obtained.

$$\text{FIM}_{\mathbf{u}} = -E\left[\left(\frac{\partial^2 \ln p(\mathbf{f} | \mathbf{u})}{\partial \mathbf{u} \partial \mathbf{u}^T}\right)\right] = \frac{\partial \mathbf{f}^T}{\partial \mathbf{u}} \mathbf{Q}_d^{-1} \left(\frac{\partial \mathbf{f}}{\partial \mathbf{u}}\right)^T, \quad (6)$$

where

$$\frac{\partial \mathbf{f}^T}{\partial \mathbf{u}} = \left[\frac{(\mathbf{u} - \mathbf{a}_1)(\mathbf{u} - \mathbf{a}_1)^T \mathbf{v}_1}{\|\mathbf{u} - \mathbf{a}_1\|^3} - \frac{\mathbf{v}_1}{\|\mathbf{u} - \mathbf{a}_1\|} - \dots \right. \\ \left. - \frac{(\mathbf{u} - \mathbf{a}_M)(\mathbf{u} - \mathbf{a}_M)^T \mathbf{v}_M}{\|\mathbf{u} - \mathbf{a}_M\|^3} - \frac{\mathbf{v}_M}{\|\mathbf{u} - \mathbf{a}_M\|} \right]. \quad (7)$$

Then, CRLB(\mathbf{u}) of the target location is

$$\text{CRLB}(\mathbf{u}) = \text{FIM}_{\mathbf{u}}^{-1}. \quad (8)$$

Observation shows that $f_i^o(\mathbf{u})$ and \mathbf{u} are a highly nonlinear relationship, which is difficult to solve directly. Next, the SDP algorithm is proposed to solve this optimization problem.

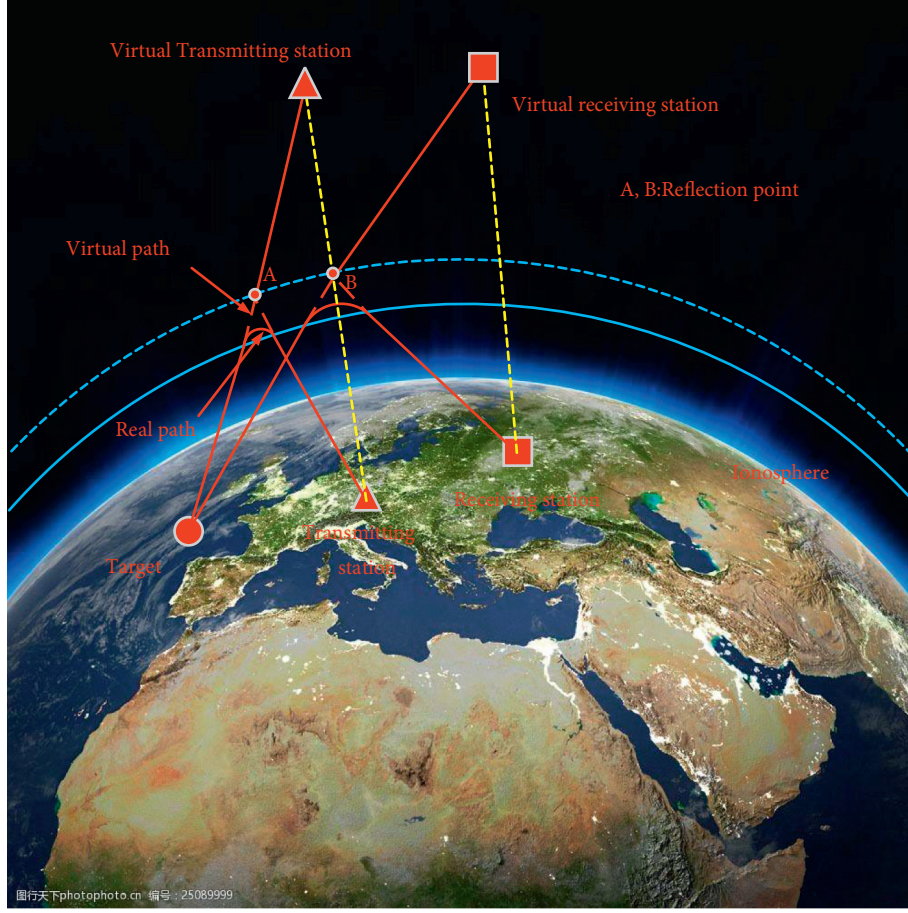


FIGURE 1: The propagation path of the signal.

3. Semidefinite Relaxation Positioning (SDP) Algorithm

Suppose the target location is $\mathbf{u}_{BLH} = [B_u, L_u, H_u]^T$ (B is the geodetic longitude, L is the geodetic latitude, and H is the altitude) and the signal station is $\mathbf{a}_i^{blh} = [B_i, L_i, H_i]^T$; then, it can convert the WGS-84 geodetic coordinate system into a rectangular coordinate system.

$$\begin{aligned} X &= (N + H)\cos(BR)\cos(LR), \\ Y &= (N + H)\cos(BR)\sin(LR), \\ Z &= (N(1 - e^2) + H)\sin(BR), \end{aligned} \quad (9)$$

where the radius of Earth is $R \approx 6370$ km, Earth's major and minor axes are $a = 6378.160$ km and $b = 6356.775$ km, $e = \sqrt{(a^2 - b^2)/a^2}$ is the first eccentricity of Earth,

$$\begin{aligned} BR &= \frac{P}{180} * B, \\ LR &= \frac{P}{180} * L, \\ N &= \frac{a}{\sqrt{(1 - e^2)\sin^2(BR)}}, \end{aligned} \quad (10)$$

Then, the left and right sides of equation (2) are simultaneously multiplied by $\|\mathbf{u}_{XYZ} - \mathbf{a}_i^{xyz}\|$ to get

$$f_i \|\mathbf{u}_{XYZ} - \mathbf{a}_i^{xyz}\| = (\mathbf{v}_i^{xyz})^T \mathbf{u}_{XYZ} - d_i + k_i n_i, \quad i = 1, \dots, M, \quad (11)$$

where $d_i = (\mathbf{v}_i^{xyz})^T \mathbf{a}_i^{xyz}$ and $k_i = \|\mathbf{u}_{XYZ} - \mathbf{a}_i^{xyz}\|$.

According to equation (11), the variable $\mathbf{m} = [\mathbf{u}_{XYZ}^T, \|\mathbf{u}_{XYZ} - \mathbf{a}_1^{xyz}\|, \dots, \|\mathbf{u}_{XYZ} - \mathbf{a}_M^{xyz}\|]^T$ can be defined; then, equation (11) can be expressed as

$$\mathbf{N}\mathbf{m} - \mathbf{d} = \mathbf{K}\mathbf{n}, \quad (12)$$

where

$$\begin{aligned} \mathbf{N} &= [\mathbf{N}_1, \mathbf{N}_2], \\ \mathbf{N}_1 &= [-\mathbf{v}_1^{xyz}, -\mathbf{v}_2^{xyz}, \dots, -\mathbf{v}_M^{xyz}], \\ \mathbf{N}_2 &= \text{diag}\{f_1, f_2, \dots, f_M\}, \\ \mathbf{d} &= [-d_1, -d_2, \dots, -d_M], \\ \mathbf{K} &= \text{diag}\{k_1, k_2, \dots, k_M\}. \end{aligned} \quad (13)$$

Adding \mathbf{m} as an optimization variable to equation (5), the original target position estimation problem becomes to minimize the following cost function:

$$\begin{aligned} \min_{\mathbf{m}, \mathbf{u}_{XYZ}} (\mathbf{N}\mathbf{m} - \mathbf{d})^T \mathbf{Q}^{-1} (\mathbf{N}\mathbf{m} - \mathbf{d}) \\ \text{s.t. } \mathbf{m}(n+i) = \|\mathbf{u}_{XYZ} - \mathbf{a}_i^{xyz}\|, \end{aligned} \quad (14)$$

where $\mathbf{Q} = \mathbf{KQ}_a\mathbf{K}^T$ is the optimal weighting matrix and n is the coordinate dimension.

Then, a new matrix $\mathbf{M} = \mathbf{m}\mathbf{m}^T$ is defined, and it will be added as an optimization condition to the optimization problem.

And according to Cauchy's inequality,

$$\begin{aligned} \mathbf{M}(n+i, n+j) &= \|\mathbf{u}_{XYZ} - \mathbf{a}_i^{xyz}\| \|\mathbf{u}_{XYZ} - \mathbf{a}_j^{xyz}\| \\ &\geq |(\mathbf{u}_{XYZ} - \mathbf{a}_i^{xyz})^T (\mathbf{u}_{XYZ} - \mathbf{a}_j^{xyz})| \\ &= |\mathbf{u}_{XYZ}^T \mathbf{u}_{XYZ} - (\mathbf{a}_i^{xyz})^T \mathbf{u}_{XYZ} \\ &\quad - (\mathbf{a}_j^{xyz})^T \mathbf{u}_{XYZ} + (\mathbf{a}_i^{xyz})^T \mathbf{a}_j^{xyz}|. \end{aligned} \quad (15)$$

In addition, $\mathbf{M} = \mathbf{m}\mathbf{m}^T$ will be relaxed into two constraints [22].

$$\mathbf{M} = \mathbf{m}\mathbf{m}^T \Leftrightarrow \begin{cases} \begin{bmatrix} \mathbf{M} & \mathbf{m} \\ \mathbf{m}^T & 1 \end{bmatrix} \succ 0, \\ \text{rank}(\mathbf{M}) = 1. \end{cases} \quad (16)$$

Among them, only $\text{rank}(\mathbf{M}) = 1$ is a nonconvex constraint; then, the constraint can be omitted [6], so a convex SDP problem can be obtained.

$$\begin{aligned} \min_{\mathbf{m}, \mathbf{u}_{XYZ}, \mathbf{M}} F &= \text{tr}(\mathbf{N}^T \mathbf{Q}^{-1} \mathbf{N}\mathbf{M}) - 2\mathbf{d}^T \mathbf{Q}^{-1} \mathbf{N}\mathbf{m} \\ \text{s.t. } \mathbf{M}(n+i, n+i) &= \text{tr}(\mathbf{M}(1:n, 1:n)) - 2(\mathbf{a}_i^{xyz})^T \mathbf{u}_{XYZ} \\ &\quad + (\mathbf{a}_i^{xyz})^T \mathbf{a}_i^{xyz} \\ \mathbf{M}(n+i, n+j) &= \left| \begin{array}{l} \text{tr}(\mathbf{M}(1:n, 1:n)) - (\mathbf{a}_i^{xyz})^T \mathbf{u}_{XYZ} \\ -(\mathbf{a}_j^{xyz})^T \mathbf{u}_{XYZ} + (\mathbf{a}_i^{xyz})^T \mathbf{a}_j^{xyz} \end{array} \right| \\ &\quad i, j = 1, \dots, M, i < j \\ \mathbf{m}(1:n) &= \mathbf{u}_{XYZ} \\ \begin{bmatrix} \mathbf{M} & \mathbf{m} \\ \mathbf{m}^T & 1 \end{bmatrix} &\succ 0. \end{aligned} \quad (17)$$

The optimal solution $\{\hat{\mathbf{m}}, \hat{\mathbf{u}}_{XYZ}, \hat{\mathbf{M}}\}$ is obtained by solving equation (17). Observation shows that the final position estimate of the target is included in both $\hat{\mathbf{u}}_{XYZ}$ and $\hat{\mathbf{M}}(1:n)$, the rank-one approximation method can be used to decompose $\hat{\mathbf{M}}(1:n)$, and the final estimated position $\hat{\mathbf{u}}_{XYZ}$ can be obtained by combining the two information.

Finally, the target position $\hat{\mathbf{u}}_{XYZ}$ can be converted into the geodetic coordinate system.

$$\begin{aligned} L &= \arctan\left(\frac{Y}{X}\right) * \frac{180}{\pi} + 180, \\ B &= \arctan\left(\frac{Z}{\sqrt{X^2 + Y^2}} * (1 - e^2)\right) * \frac{180}{\pi}, \\ H &= \sqrt{\frac{X^2 + Y^2 + Z^2}{(1 - e^2)^2} - a}. \end{aligned} \quad (18)$$

Then, the target final position coordinates are $\tilde{\mathbf{u}}_{BLH} = [B_u, L_u, H_u]^T$, but in this paper, the ship's goal is considered, $H_u = 0$ (Algorithm 1).

4. Simulation Results

In this paper, there are four transmitting stations and four receivers (the first four are transmitting stations and the last four are receiving stations). The geodetic coordinates and velocities of all stations are

$$\begin{aligned} \mathbf{a}_1^{blh} &= [30.41^\circ \text{N}, 111.51^\circ \text{E}, 0], \mathbf{v}_1^{xyz} = \left[\frac{25 \text{ km}}{h}, \frac{10 \text{ km}}{h}, 0 \right], \\ \mathbf{a}_2^{blh} &= [32.44^\circ \text{N}, 114.76^\circ \text{E}, 0], \mathbf{v}_2^{xyz} = \left[\frac{-20 \text{ km}}{h}, \frac{10 \text{ km}}{h}, 0 \right], \\ \mathbf{a}_3^{blh} &= [31.95^\circ \text{N}, 112.54^\circ \text{E}, 0], \mathbf{v}_3^{xyz} = \left[\frac{10 \text{ km}}{h}, \frac{-5 \text{ km}}{h}, 0 \right], \\ \mathbf{a}_4^{blh} &= [32.31^\circ \text{N}, 105.42^\circ \text{E}, 0], \mathbf{v}_4^{xyz} = \left[\frac{15 \text{ km}}{h}, \frac{-15 \text{ km}}{h}, 0 \right], \\ \mathbf{a}_5^{blh} &= [36.32^\circ \text{N}, 108.90^\circ \text{E}, 0], \mathbf{v}_5^{xyz} = \left[\frac{5 \text{ km}}{h}, \frac{5 \text{ km}}{h}, 0 \right], \\ \mathbf{a}_6^{blh} &= [28.67^\circ \text{N}, 111.03^\circ \text{E}, 0], \mathbf{v}_6^{xyz} = \left[\frac{10 \text{ km}}{h}, \frac{-15 \text{ km}}{h}, 0 \right], \\ \mathbf{a}_7^{blh} &= [34.05^\circ \text{N}, 110.52^\circ \text{E}, 0], \mathbf{v}_7^{xyz} = \left[0, \frac{-5 \text{ km}}{h}, 0 \right], \\ \mathbf{a}_8^{blh} &= [30.75^\circ \text{N}, 116.35^\circ \text{E}, 0], \mathbf{v}_8^{xyz} = \left[\frac{10 \text{ km}}{h}, 0, 0 \right], \end{aligned} \quad (19)$$

and $\mathbf{u}_{BLH} = [35.41^\circ \text{E}, 121.51^\circ \text{N}, 0]$ is the initial target coordinate. Since the detection range of the DMOTHR can reach 800 km–2000 km [3], this paper sets the minimum distance between the target and the stations as 850 km and the maximum distance as 1500 km. Since the project is still in the early stage of research, the actual transceiver station site has not been determined, and the transceiver station sites used in this article are all simulated data.

This paper compares the positioning performance of the proposed SDP algorithm with the two-step weighted least squares (2WLS) algorithm [23]. In the simulation, all re-

Input: the position \mathbf{a}_i^{blh} , the speed \mathbf{v}_i^{blh} of the transceiver station, and the initial position \mathbf{u}_{BLH}^0 .
Output: the target final position coordinates are $\tilde{\mathbf{u}}_{BLH} = [B_u, L_u, H_u]^T$.

- (1) Convert the WGS-84 geodetic coordinate system into a rectangular coordinate system.
- (2) Get the Doppler frequency \mathbf{f} .
- (3) Deform and simplify equation (2) to get optimization problem (12).
- (4) Use the SDPT3 method to get $\{\hat{\mathbf{m}}, \hat{\mathbf{u}}_{XYZ}, \hat{\mathbf{M}}\}$.
- (5) If $\text{rand}(\hat{\mathbf{M}}(1:n)) = 1$
- (6) $\tilde{\mathbf{u}}_{XYZ} = \hat{\mathbf{u}}_{XYZ}$.
- (7) else
- (8) decompose $\hat{\mathbf{M}}(1:n) \Rightarrow \bar{\mathbf{u}}_{XYZ}$
- (9) if $F(\bar{\mathbf{u}}_{XYZ}) < F(\hat{\mathbf{u}}_{XYZ})$
- (10) $\tilde{\mathbf{u}}_{XYZ} = \bar{\mathbf{u}}_{XYZ}$
- (11) else
- (12) $\tilde{\mathbf{u}}_{XYZ} = \hat{\mathbf{u}}_{XYZ}$
- (13) end if
- (14) end if
- (15) Coordinate conversion $\tilde{\mathbf{u}}_{XYZ} \Rightarrow \tilde{\mathbf{u}}_{BLH}$
- (16) $H_u = 0$
- (17) The target final position coordinates are $\tilde{\mathbf{u}}_{BLH} = [B_u, L_u, 0]^T$.

ALGORITHM 1: The pseudo-code of the algorithm is to get the target position $\tilde{\mathbf{u}}_{BLH} = [B_u, L_u, H_u]^T$.

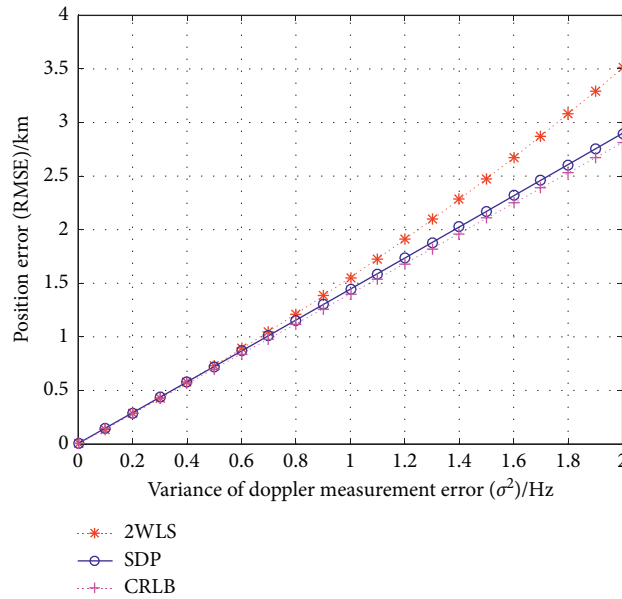


FIGURE 2: The relationship between Doppler frequency error and positioning accuracy. The height of the reflected ionosphere of the observation station is $H_{a1} = 90$ km, $H_{a2} = 92$ km, $H_{a3} = 95$ km, $H_{a4} = 105$ km, $H_{a5} = 100$ km, $H_{a6} = 102$ km, $H_{a7} = 104$ km, and $H_{a8} = 110$ km.

ceiving stations perform Doppler frequency measurement every 5 s, and a total of 10 measurements are performed; then, the SDP algorithm in this paper is used to locate the target. Since there may also be errors in the process of measuring the height of the ionosphere [24], this paper will simulate in three cases: based on the Doppler frequency measurement error, based on the ionospheric height measurement error, and based on Doppler frequency and ionospheric height measurement error.

Figure 2 shows the simulation of positioning accuracy based on Doppler frequency error. It is assumed that each Doppler frequency measurement error n_i is an independent

and uniformly distributed Gaussian variable, and the variance is σ^2 ; then, the covariance matrix is $\mathbf{Q}_d = \sigma^2 \mathbf{I}$. It can be seen from Figure 2 that the positioning accuracy of the 2WLS algorithm and the SDP algorithm is almost the same in the error range of 0–0.6 Hz, but as the error becomes larger and larger, the positioning performance of the SDP algorithm is much better than that of the 2WLS algorithm. Moreover, SDP algorithm can basically reach the CRLB within the range of 0–2 Hz of Doppler frequency measurement error.

Figure 3 shows the simulation of positioning accuracy based on the ionospheric reflection height error. It can be

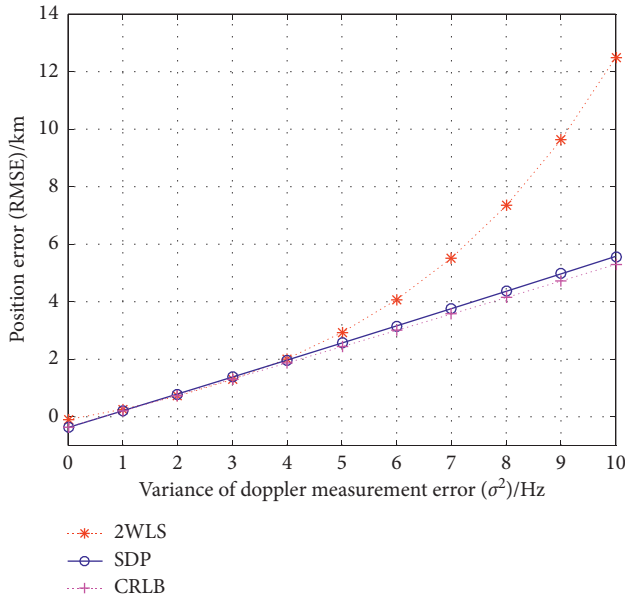


FIGURE 3: The relationship between the reflected ionospheric height error and positioning accuracy. The Doppler frequency error is set to 1 Hz, the basic ionospheric reflection height of all observing stations is 100 km, which is in the E layer, and the error range is 0–10 km.

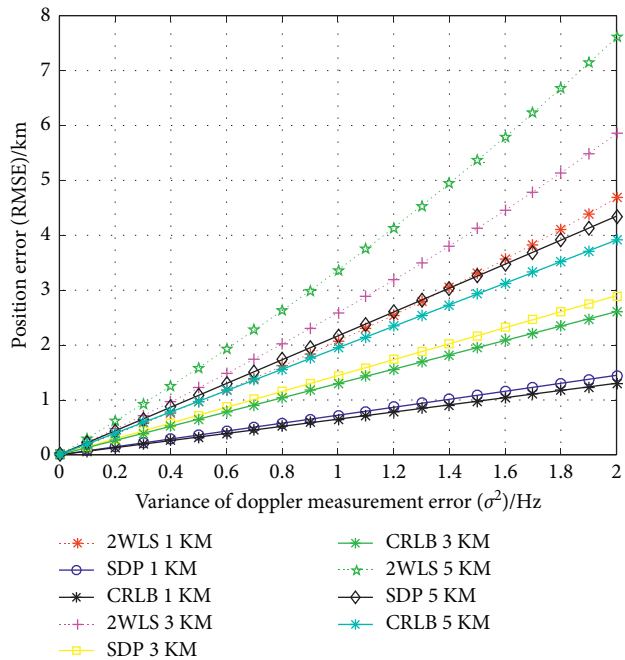


FIGURE 4: The relationship between the Doppler frequency error and ionospheric height error. The basic reflection ionosphere height of all observing stations is 105 km.

seen from Figure 3 that the positioning accuracy of the two algorithms is equivalent within the error range of 0–4 km, but as the error increases, the positioning accuracy performance of the SDP algorithm is much better than that of the 2WLS algorithm, and the increase of the 2WLS algorithm is an exponential function.

Figure 4 shows a simulation of positioning accuracy based on both Doppler frequency error and ionospheric height error. The conclusion from Figure 4 is that the positioning accuracy of the error range of the ionosphere height of 1 km is better than that of 3 km and 5 km under the condition of a certain Doppler frequency error, which means that the lower the reflection point of the ionosphere, the better the positioning accuracy; on the contrary, when the ionospheric height error is constant, the positioning accuracy will become worse as the Doppler frequency error increases. In general, the positioning accuracy of the SDP algorithm is better than that of the 2WLS algorithm regardless of the Doppler frequency error or the ionospheric height error.

5. Conclusion

This paper studies the positioning of ships on the sea by a DMOTHR system. Based on the Doppler frequency measurement error and the ionospheric height measurement error, the SDP algorithm is used for the highly nonlinear positioning optimization problem. The result of better positioning performance compared with 2WLS algorithm is obtained, and the SDP algorithm enriches the positioning algorithm of the OTHR to a certain extent, but this paper only studies the single-target problem; it will be extended to the multitarget positioning optimization problem in the future.

Data Availability

The MATLAB codes used in this study are available from the first author upon request (renfangyu921@163.com).

Conflicts of Interest

The authors declare that there are no conflicts of interest regarding the publication of this paper.

Acknowledgments

This research was funded by the National Natural Science Foundation of China (no. 61671333), the Natural Science Foundation of Hubei Province (no. 2014CFA093), the Fundamental Research Funds for the Central Universities (nos. 2042019K50264, 2042019GF0013, and 2042020gf0003), and the Fundamental Research Funds for the Wuhan Maritime Communication Research Institute (no. 2017J-13).

References

- [1] S. Kingsley and S. Quegan, "Over-the-horizon radar," *Understanding Radar Systems*, IET Digital Library, Stevenage, UK, 1999.
- [2] D. Jia, B. Zhang, and J. Xie, "Adaptive processing method for interference cancellation in sky-wave OTHR," *Journal of Engineering*, vol. 2019, no. 21, pp. 8103–8106, 2019.
- [3] M. Mostafa Nazari and R. Mohseni, "Waveform design with application in over-the-horizon skywave radar," *Shiyou Kantan Yu Kaiifa/petroleum Exploration & Development*, vol. 42, no. 4, pp. 507–511, 2015.

- [4] Z. Luo, Z. He, X. Chen, and K. Lu, "Target location and height estimation via multipath signal and 2D array for sky-wave over-the-horizon radar," *IEEE Transactions on Aerospace and Electronic Systems*, vol. 52, no. 2, pp. 617–631, 2016.
- [5] L. Yang, H. Gao, Y. Ling, and B. Li, "Localization method of wide-area distribution multistatic sky-wave over-the-horizon radar," *IEEE Geoscience and Remote Sensing Letters*, vol. 18, no. 99, pp. 1–5, 2020.
- [6] M. R. Dianat, J. Taban, and V. Sedighi, "Target localization using least squares estimation for MIMO radars with widely separated antennas," *IEEE Transactions on Aerospace and Electronic Systems*, vol. 49, no. 4, pp. 2730–2741, 2014.
- [7] Q. He, R. S. Blum, and A. M. Haimovich, "Noncoherent MIMO radar for location and velocity estimation: more antennas means better performance," *IEEE Transactions on Signal Processing*, vol. 58, no. 7, pp. 3661–3680, 2010.
- [8] A. Noroozi, A. H. Oveis, and M. A. Sebt, "Iterative target localization in distributed MIMO radar from bistatic range measurements," *IEEE Signal Processing Letters*, vol. 24, no. 11, p. 1, 2017.
- [9] Y. Zhao, D. Hu, Z. Liu, and Y. Zhao, "Calibrating the transmitter and receiver location errors for moving target localization in multistatic passive radar," *IEEE Access*, vol. 7, 2019.
- [10] Y. Zhang and K. C. Ho, "Multistatic localization in the absence of transmitter position," *IEEE Transactions on Signal Processing*, vol. 67, no. 18, pp. 4745–4760, 2019.
- [11] Y. D. Zhang, J. J. Zhang, M. G. Amin, and B. Himed, "Instantaneous altitude estimation of manoeuvring target in over-the-horizon radar exploiting multipath Doppler signatures," *EURASIP Journal on Applied Signal Processing*, vol. 2013, no. 1, 13 pages, Article ID 100, 2013.
- [12] K. C. Ho, X. Lu, and L. Kovavisaruch, "Source localization using TDOA and FDOA measurements in the presence of receiver location errors: analysis and solution," *IEEE Transactions on Signal Processing*, vol. 55, no. 2, pp. 684–696, 2007.
- [13] Y. Le Yang and K. C. Ho, "An approximately efficient TDOA localization algorithm in closed-form for locating multiple disjoint sources with erroneous sensor positions," *IEEE Transactions on Signal Processing*, vol. 57, no. 12, pp. 4598–4615, 2009.
- [14] D. Wang, J. Yin, R. Liu, H. Yu, and Y. Wang, "Performance analysis and improvement of direct position determination based on Doppler frequency shifts in presence of model errors: case of known waveforms," *Multidimensional Systems and Signal Processing*, vol. 30, no. 2, pp. 749–790, 2019.
- [15] J. Yin, D. Wang, Y. Wu, and R. Liu, "Direct localization of multiple stationary narrowband sources based on angle and Doppler," *IEEE Communications Letters*, vol. 21, no. 12, pp. 2630–2633, 2017.
- [16] D. Wang and G. Zhang, "A direct localization method for moving narrowband source based on Doppler frequency shifts," *Acta Electronica Sinica*, vol. 45, no. 3, Article ID 591, 2017.
- [17] S. Zhenqiang, S. Genfu, and L. Huaping, "Semidefinite programming for NLOS error mitigation in TDOA localization," *IEEE Communications Letters*, vol. 22, 2017.
- [18] Q. He, X. Li, Z. He, and R. S. Blum, "MIMO-OTH radar: signal model for arbitrary placement and signals with non-point targets," *IEEE Transactions on Signal Processing*, vol. 63, no. 7, pp. 1846–1857, 2015.
- [19] Y.-T. Chan and F. L. Jardine, "Target localization and tracking from Doppler-shift measurements," *IEEE Journal of Oceanic Engineering*, vol. 15, no. 3, pp. 251–257, 1990.
- [20] Y. Zou, Q. Wan, and H. Liu, "Semidefinite programming for tdoa localization with locally synchronized anchor nodes," in *Proceedings of the 2018 IEEE International Conference on Acoustics, Speech and Signal Processing (ICASSP)*, pp. 3524–3528, Calgary, AB, Canada, April 2018.
- [21] W. Li, W. Peng, L. Peng, Y. Ma, and Y. Li, "Semidefinite programming algorithm with TDOA and FDOA measurements based on WGS-84 earth model," *Acta Aeronautica et Astronautica Sinica*, vol. 38, no. 7, 2017.
- [22] Y. Du, P. Wei, and H. Zhang, "Semidefinite programming approach for TDOA/GROA based source localization," *Journal of Systems Engineering and Electronics*, vol. 26, no. 4, pp. 680–687, 2015.
- [23] F. Ren, H. Gao, and L. Yang, "Distributed multistatic sky-wave over-the-horizon radar based on the Doppler frequency for marine target positioning," *Electronics*, vol. 10, no. 12, Article ID 1472, 2021.
- [24] H. Li, C. Xue, Z. Chen, and J. Hu, "Maneuvering target detection algorithm based on hankel matrix decomposition in over-the-horizon radar," *Dianzi Yu Xinxin Xuebao/Journal of Electronics and Information Technology*, vol. 40, no. 3, pp. 541–547, 2018.